Parallel-Shift Tomosynthesis for Orthopedic Applications

Christoph Luckner[a,b], Stefan Sesselmann[c], Thomas Mertelmeier[a], Andreas Maier[b], and Ludwig Ritschl[a]

[a]Siemens Healthcare GmbH, Forchheim
[b]Chair of Pattern Recognition, University Erlangen-Nuremberg
[c]Innovative Concepts and Technologies in Healthcare, OTH Amberg-Weiden

ABSTRACT

The upsurge in interest of digital tomosynthesis is mainly caused by breast imaging; however, it finds more and more attention in orthopedic imaging as well. Offering a superior in-plane resolution compared to CT imaging and the additional depth information compared to conventional 2-D X-ray images, tomosynthesis may be an interesting complement to the other two imaging modalities. Additionally, a tomosynthesis scan is likely to be faster and the radiation dose is considerably below that of a CT. Usually, a tomosynthetic acquisition focuses only on one body part as the common acquisition techniques restrict the field-of-view. We propose a method which is able to perform full-body acquisitions with a standard X-ray system by shifting source and detector simultaneously in parallel planes without the need to calibrate the system beforehand. Furthermore, a novel aliasing filter is introduced which addresses the impact of the non-isotropic resolution during the reconstruction. We provide images obtained by filtered as well as unfiltered backprojection and discuss the influence of the scanning angle as well as the reconstruction filter on the reconstructed images. We found from the experiments that our method shows promising results especially for the imaging of anatomical structures which are usually obscured by each other since the depth resolution allows to distinguish between these structures. Additionally, as of the high isotropic in-plane spatial resolution of the tomographic volume, it is easily possible to perform precise measurements which are a crucial task, e. g. during the planning of orthopedic surgeries or the assessment of pathologies like scoliosis or subtle fractures.

Keywords: Digital Tomosynthesis, Tomography, Aliasing filter, Reconstruction, Full-body imaging, Orthopedics

1. INTRODUCTION

Digital tomosynthesis is a tomographic imaging technique using flat panel detectors, which allows creating multiple tomographic slices through the object [1]. However, it only provides incomplete three-dimensional (3-D) information which means that those reconstructions suffer from a relatively poor depth resolution compared to CT imaging because of the limited acquisition angle. Yet, digital tomosynthesis provides excellent visibility of fine structures due to its high in-plane spatial resolution, necessary for the assessment of high contrast structures e. g. bone fractures, synostosis status or bone and joint structures, which can be difficult to assess in conventional 2-D radiographs [2–5]. Additionally, measurement-based procedures like the assessment of scoliotic spines or the planning of implants might benefit from the geometrical correctness of tomosynthetic imaging. The most common acquisition geometries are parallel-path motion (X-ray tube moves in a plane parallel to the detector which is either fixed or moves in opposing direction of the tube), full-isocentric motion (source and detector are fixed rigidly and move in a circular path around the patient) and partial-isocentric motion (detector remains static and the tube moves in an arc trajectory around the patient) [6]. However, all these techniques have in common that they limit the available field-of-view. Currently, mainly two approaches to generate X-ray projection images of the full body (or body parts like the full spine or the entire leg) are used: slot scanning and the source-tilting technique.

The first uses only a small slot which is irradiated and combines the individual projection images into one image. This technique has the advantage that only little scattered radiation is produced and hence, the images

christoph.luckner@fau.de

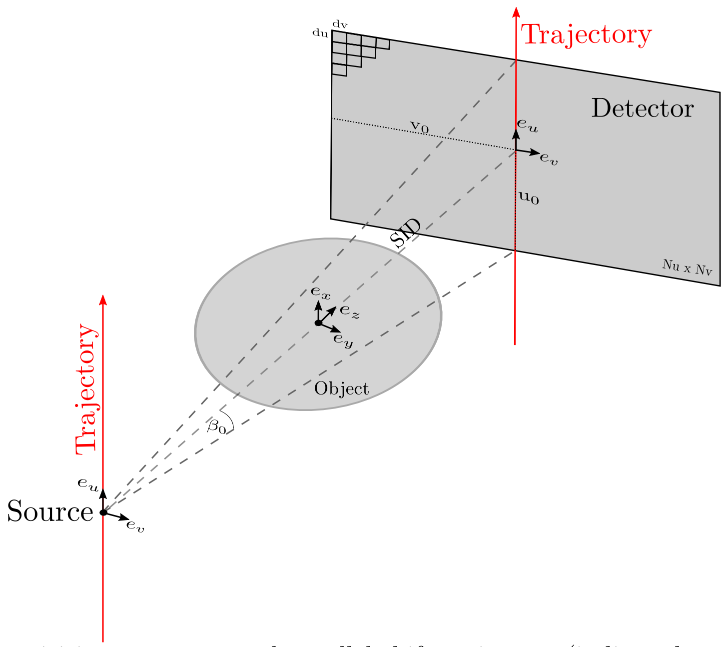

Figure 1: Acquisition geometry and parallel-shift trajectory (indicated as red arrows)

can be acquired at very low dose [7]. The source-tilting technique, on the other hand, is characterized by a source which remains static at a certain region of interest of the patient and is tilted such that the rays always hit the full detector while the detector moves along the height of the patient. To cope with distortion and magnification the SID is usually chosen to be as large as possible [8].

The parallel-shift tomosynthesis is characterized by a simultaneous movement of X-ray source and detector along a line trajectory. The acquired projections form the basis for the reconstruction of a 3-D representation of the scanned object [9]. It allows the acquisition of a full-body in lying or standing position as well as functional imaging even with a standard X-ray system capable of dynamic acquisition protocols in a single scanning procedure. Because the reconstructed slices do not suffer from magnification or distortion, they could be used for surgical planning or the assessment of pathologies since measurements are easily possible even without the need of a calibration object.

However, since the reading time of those images is increased compared to plain 2-D X-rays, a synthetic radiograph can be created based on the 3-D reconstruction by performing a simple parallel or a spline-based projection of the slices [10].

2. MATERIALS AND METHODS

In the following, the image acquisition geometry, the novel slice thickness dependent aliasing filter, as well as the image reconstruction using filtered as well as unfiltered backprojection in combination with a voxel-specific weighting will be outlined. In the end, the carried out experiments using simulated as well as real data are described.

2.1 Image Acquisition Geometry

The acquisition geometry is illustrated in Figure 1. The distance between source and detector is denoted as SID. Nu and Nv is the number of pixels in u- and v direction, respectively. The corresponding pixel pitch is denoted as du and dv and is assumed to be isotropic. The tomosynthesis angle β is defined as

$$\beta = 2 \cdot \beta_0 = 2 \cdot \arctan\left(\frac{\mathrm{Nu} \cdot \mathrm{du}}{2 \cdot \mathrm{SID}}\right). \tag{1}$$

The used line trajectory, i. e. source and detector moving simultaneously in parallel planes, is indicated with red arrows [9].

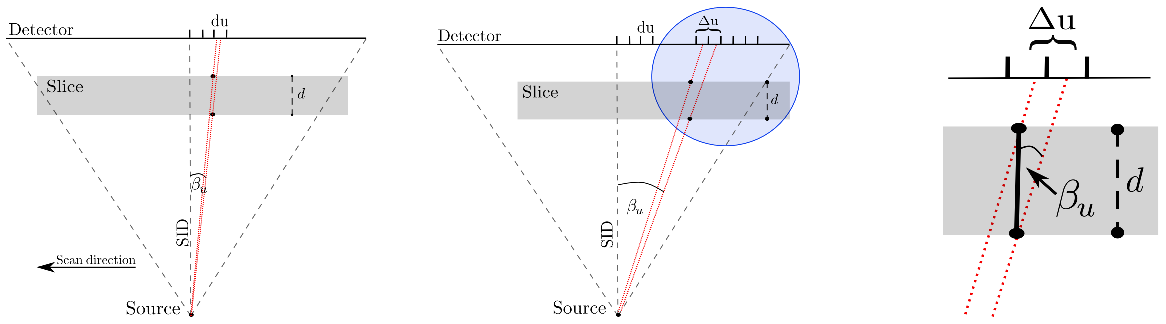

(a) Initial projection (b) Projection after translation (c) Detailed view (indicated by the blue circle in (b))

Figure 2: Geometrical representation of the slice thickness dependent aliasing filter

2.2 Slice Thickness Dependent Aliasing Filter

The effect of signals becoming indistinguishable when they are sampled is commonly referred to as aliasing. In image processing, these aliasing artifacts occur when a high-resolution image is represented at a lower resolution. Since we deal with a non-isotropic resolution during the reconstruction, as illustrated in Figure 2, we propose to apply an aliasing filter in order to avoid aliasing artifacts, which is dependent on the tomosynthesis angle β and the desired slice thickness d to the projection [11]. We assume that SID $\gg d$, which yields that the rays can be treated as parallel within a slice, as indicated in Figure 2c. The aliasing filter is designed as a Gaussian kernel K

$$K(u) = \frac{1}{\sigma_\beta\sqrt{2\pi}} e^{-\frac{1}{2}\left(\frac{u-u_0}{\sigma_\beta}\right)^2}, \tag{2}$$

with u_0 as middle pixel of the detector, and a standard deviation σ_β based on the acquisition angle β

$$\sigma_{\beta_u} = c \cdot \underbrace{\tan(\beta_u) \cdot d}_{\Delta u} + \varepsilon_0, \tag{3}$$

with β_u as angle between the central ray and the ray hitting the detector at the pixel with coordinate u and d as slice thickness of the reconstruction. Δu denotes the length in u-direction over which a point in the slice is distributed on the detector and c a constant to adjust the magnitude of the filter. Furthermore, we introduce the additive constant $\varepsilon_0 \gtrapprox 0$ to avoid a division by zero. Hence, the middle area of the projections (i. e. where the rays hit the detector approximately perpendicularly) are filtered with a kernel with a small standard deviation (see Figure 2a), whereas the kernel becomes broader at the outer areas of the detector (see Figure 2b).

Figure 3 illustrates the individual filtering steps and shows a raw projection image, the same image after applying the ramp filter as well as after applying the ramp and aliasing filter. It can be seen that the ramp filter is a high-pass filter intensifying high frequencies in the image. The aliasing filter, on the other hand, introduces a blurring to deal with high frequencies which can not be resolved by the system due to its non-isotropic resolution which helps to reduce aliasing in the reconstructed slices.

2.3 Reconstruction

As stated before, tomosynthesis is characterized by incomplete data acquisition, which means that it fails to provide a complete and isotropic 3-D imaging of the scanned object. The reconstruction itself is performed using the widely-used backprojection algorithm [1,12,13]. We use unfiltered as well as filtered backprojection. For the latter, the well-known Ramp filter is applied along the scanning-direction (i. e. in u-direction), which weights each projection with the inverse of the sampling density to avoid a blurred reconstruction. For additional noise reduction, we applied the Hanning window as apodization filter [14]. Subsequently, the formerly introduced aliasing filter is applied to the projections. Then, a voxel-driven perspective reconstruction of the (un-)filtered projections is performed based on a simple look-up operation. In order to take the varying illumination of each voxel into account, we additionally apply a voxel-specific weighting based on the hit count of each voxel [15].

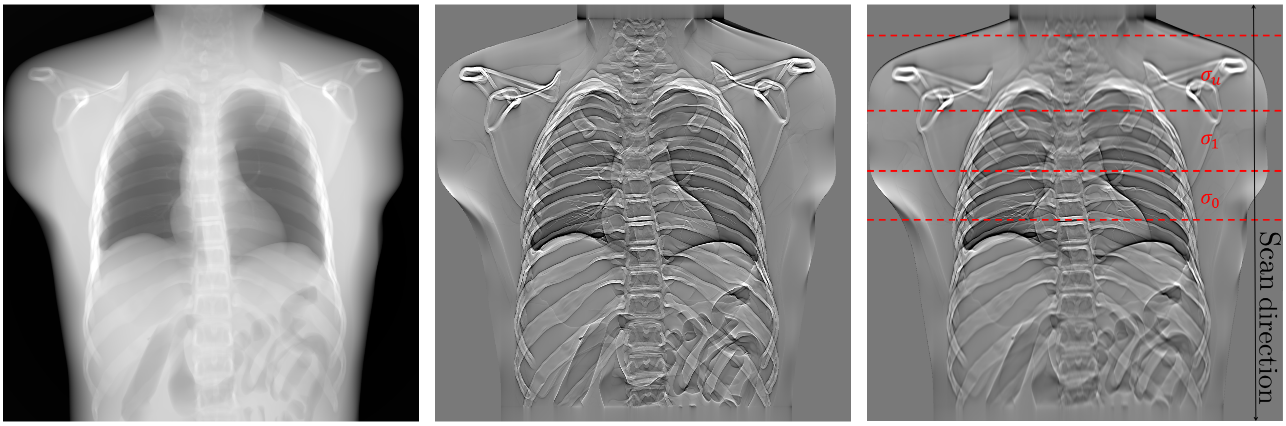

(a) Raw projection data (b) ... after ramp filter (c) ... after aliasing filter

Figure 3: Raw projection and the results after both filtration steps

During the reconstruction, we assume a perfect line trajectory and equidistant spacing between the acquired projections, hence, it is possible to perform the reconstruction of the scanned object without having to calibrate the system beforehand. However, to improve the quality of the reconstructions a calibration using either an axially extended calibration phantom covering the entire scanning range or an image-based registration approach would be possible assuming that the intrinsic parameters of the system are known and remain constant during the scan.

2.4 Experiments

To explore our idea, we acquired simulated as well as real data. For a first proof of concept, we simulated a scan with a female XCAT full-body phantom [16]. In total 140 noise-free projections (120 kV, 1440x1440 pixel á 0.296 mm with SID = 180 cm and SOD = 140 cm) in a. p. as well as lateral view were acquired using the presented trajectory and were used for reconstruction.

In a second step, we implemented the presented trajectory on a twin-robotic X-ray scanner Multitom Rax (Siemens Healthcare) [17] which is equipped with two ceiling mounted fully motorized robotic arms and is able to perform scans along a defined trajectory. A full-body phantom was attached to a patient support and scanned in an upright position in a. p. as well as in lateral view. Each acquisition consists of 79 projections (120 kV, 8.5 mAs, 1436x1420 pixel á 0.296 mm with SID = 140 cm and SOD = 100 cm).

In order to evaluate the influence of the scanning angle β on the depth resolution of the reconstructed dataset, we simulated different scanning angles. Therefore, we collimated the irradiated detector area ranging from slot sizes of 5 cm to 40 cm to obtain different scanning angles. The slot sizes and their corresponding scanning angles are outlined in Table 1.

Table 1: Investigated slot sizes and corresponding scanning angles

Slot size [mm]	50	100	150	200	250	300	350	400
Scanning Angle β [°]	2	4	6	8	10	12	14	16

3. RESULTS

3.1 Simulated Data

In Figure 4a a slice of the tomographic volume generated with unfiltered backprojection is shown. Figure 4b shows the simulation of a conventionally taken full-body radiograph, acquired with the earlier introduced source-tilting technique. Furthermore, a detail view of the knee is given for both imaging techniques. It can be seen that the joint gap of the knee is clearly visible in the tomographic slice whereas the conventionally stitched radiograph suffers from overlapping structures and stitching marks which impair the overall image appearance. On the

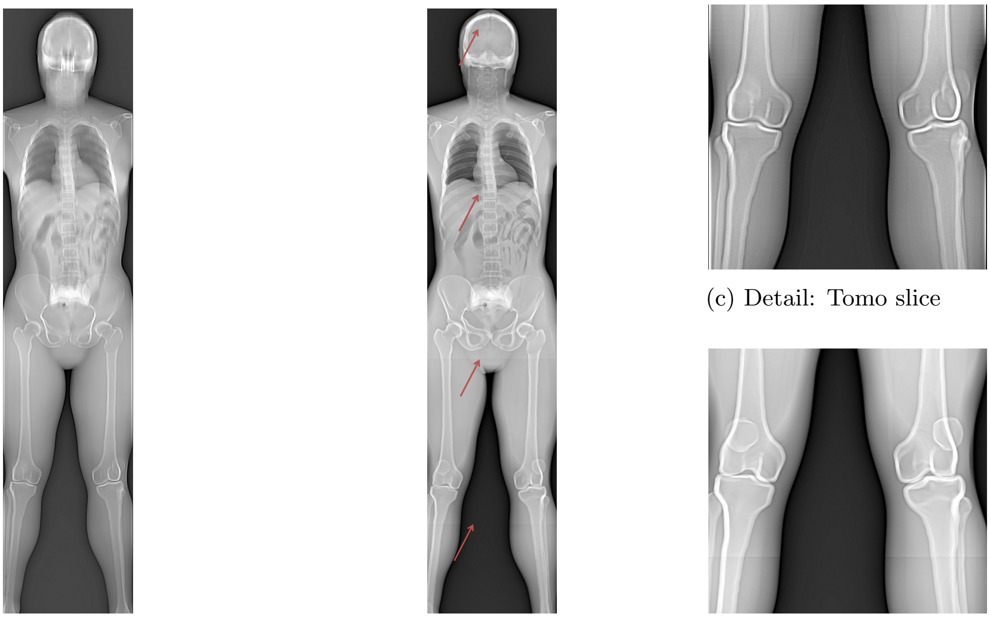

(a) Tomographic slice (b) Source-tilting technique (c) Detail: Tomo slice (d) Detail: Radiograph

Figure 4: Comparison of a tomographic slice and a conventional full-body radiograph acquired with the source-tilting technique of the XCAT phantom and a corresponding detail view of the knee joint. The stitching marks are indicated with red arrows.

other hand, the rips, as well as the cervical spine, cannot be seen as clearly in the tomographic slice as in the conventional radiograph which is due to the depth-resolved anatomic information.

3.2 Real Data

Figure 5 shows the central slice of the unfiltered backprojection reconstruction of the a. p. as well as the lateral projections with selected slot sizes as presented in Table 1. For the a. p. view, it can be seen that the thoracic spine is getting more and more blurred with increasing slot size. The same phenomenon can be observed for the shoulder and the hip in the lateral view dataset. This behavior was already subject to previous of research and is well described in the literature. In a nutshell, with increasing scanning angle, i. e. with increasing slot size, the depth resolution is getting better [18], leading to the blurred-out image impression of the anatomical structures in the presented images. For our application, this can be utilized to generate images that do not suffer from overlapping anatomical structures. For instance, it is now possible to acquire images of the spine in lateral view without having the shoulder obscuring the vertebral bodies.

Furthermore, two slices of each dataset generated with filtered backprojection are shown in Figure 6. It can be seen that the used Ramp filter acts as high-pass emphasizing especially the edges of the bones perpendicular to the scanning direction. On the other hand, edges parallel to the scanning direction vanish slightly.

4. DISCUSSION

The biggest advantage of the presented method compared to a conventional full-body X-ray acquisition is that all joint areas are perfectly visible in the reconstruction and that there are no overlaps of bones or joints. Furthermore, it is possible to distinguish between certain structures which are usually obscured by each other. Yet, the presented method has three major influencing variables that need further optimization: the scanning angle, the reconstruction filter as well as the number of projections. As already shown, the scanning angle determines the depth resolution of the reconstructed dataset - the larger the scanning angle the better the depth resolution which is beneficial for the separation of anatomical structures. However, parasitic effects like scattered radiation which usually impair the image contrast and thus the visibility of structures in the image can be dampened with a

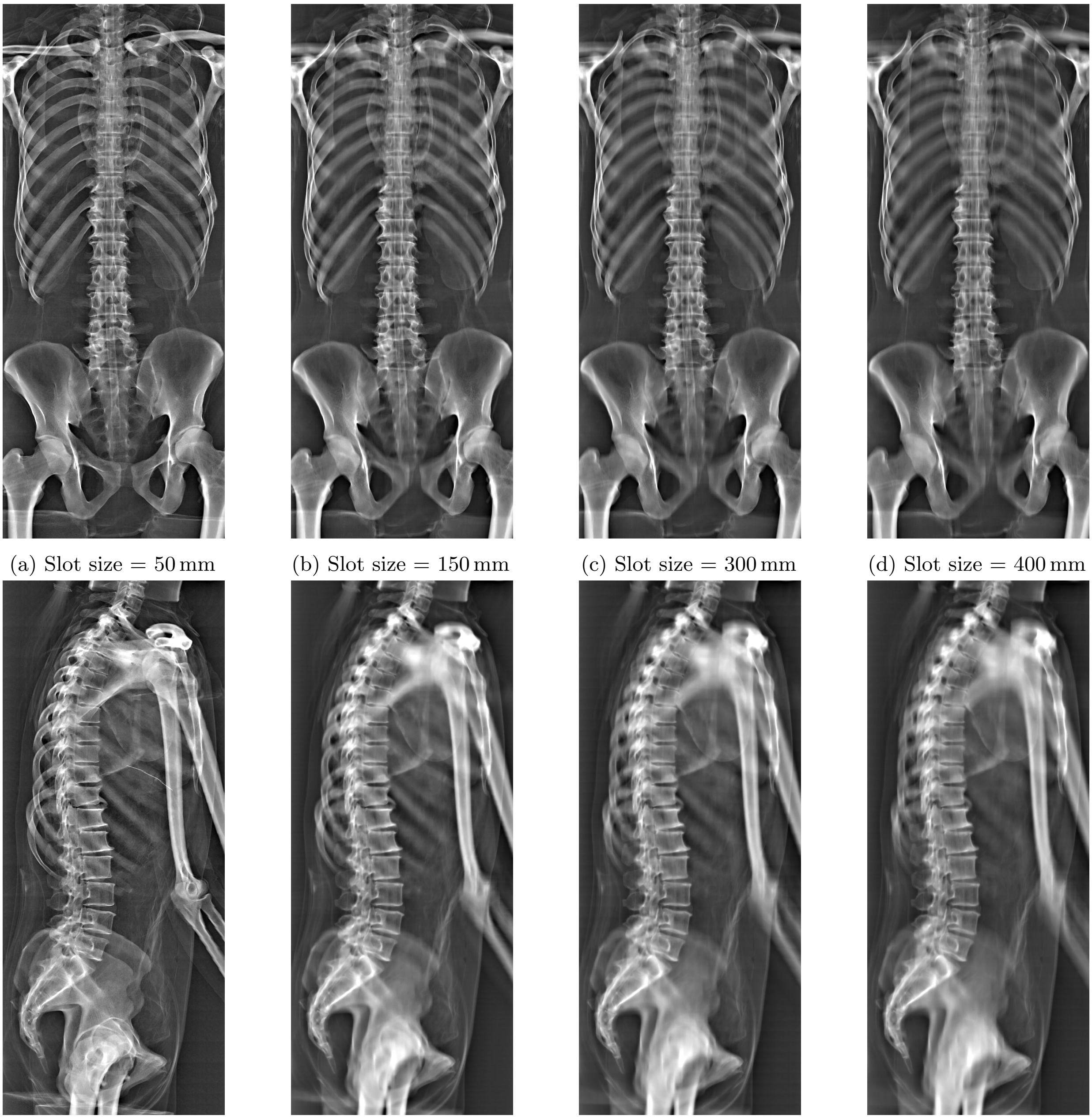

(a) Slot size = 50 mm (b) Slot size = 150 mm (c) Slot size = 300 mm (d) Slot size = 400 mm

(e) Slot size = 50 mm (f) Slot size = 150 mm (g) Slot size = 300 mm (h) Slot size = 400 mm

Figure 5: Influence of slot size (i. e. scanning angle) on the depth resolution for the a. p. (a-d) and the lateral (e-h) dataset generated with unfiltered backprojection.

smaller scanning angle. Since the irradiated area is smaller, the dose, as well as the amount of scattered radiation, is smaller compared to a full-field radiograph. Hence, it is necessary to find an optimal trade-off between the required depth resolution and the applied radiation dose, which is currently still subject to our research.

The second point that needs to be discussed is the choice of the reconstruction filter. Unfiltered backprojection suffers from a slightly blurred image impression. However, the commonly used Ramp filter is not optimal for our scanning geometry with the highly limited acquisition angle. This, for instance, is also the reason why structures parallel to the scanning direction might not be clearly visible. One solution would be to change the reconstruction algorithm to an iterative reconstruction technique which is capable to reconstruct the optimal image even in case

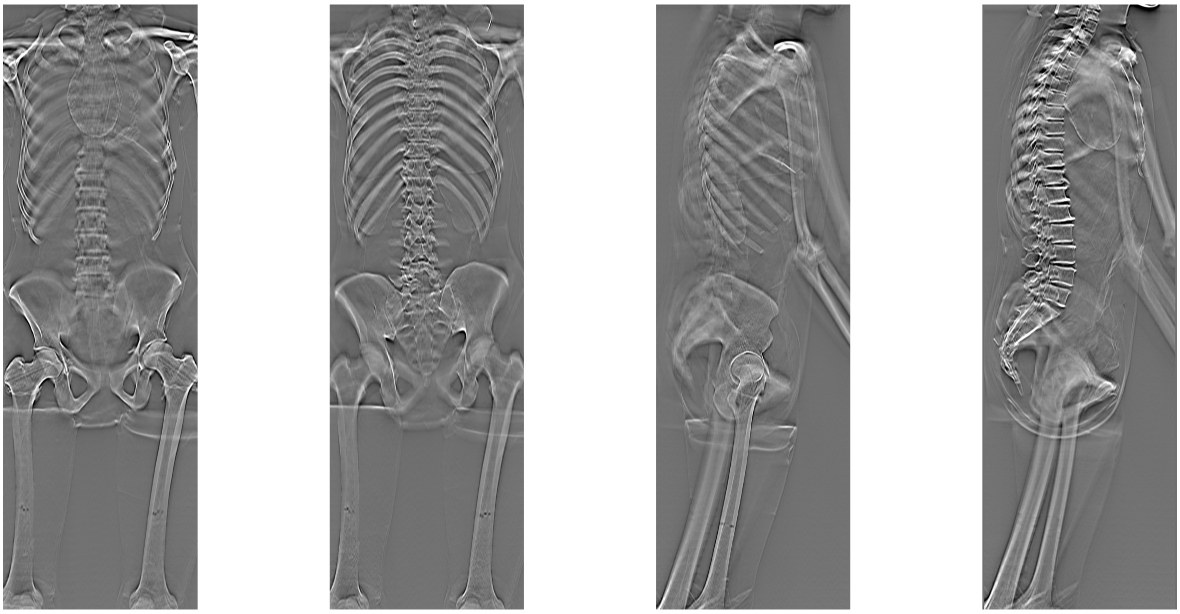

(a) Focus on hip a. p. (b) Focus on spine a. p. (c) Focus on hip lat. (d) Focus on spine lat.

Figure 6: Two exemplary slices of the a. p. (a,b) and lateral (c,d) dataset generated with filtered backprojection focusing on hip and on spine

of incomplete data yielding a better image impression but has much higher computation time. However, there are reconstruction filters like the one presented in [19] combining the image appearance of an iterative reconstruction and the speed of the filtered backprojection, which might also be beneficial for our proposed method.

In addition, also the scanning time and thus the number of projections must be considered. Currently, one scan takes about 8 seconds. We aim to optimize the scanning protocol such that an entire a. p. and lateral scan can be acquired at the same time, by finding the lowest possible number of projections which still allows a good image quality and low radiation dose at the same time.

5. CONCLUSION

The tomosynthetic reconstructions of the simulated, as well as the real projections, show promising results. For a long time, geometrically correct full-body acquisitions have only been possible with CT imaging causing a relatively high radiation exposure for the patient or with stitched radiographs which can suffer from an inhomogeneous image impression, distortion and magnification and hence rely on well-positioned calibration objects in the image to allow precise measurements. The used parallel-shift tomosynthesis addresses all issues. This acquisition trajectory, which - compared to the ones presented in [1] - only relies on a simultaneous moving detector and source along a straight line is easy to implement in a clinical environment, providing a way of low-dose geometrically correct full-body imaging in standing or lying position, even with a standard radiography or fluoroscopy system. The high in-plane spatial resolution may allow the assessment of fine structures like subtle fractures and the depth resolution even though it is limited allows separating anatomical structures. The geometrically correct representation enables measurements of distances and angles directly in the tomographic volume or synthetically created radiographs without any calibration objects.

DISCLAIMER

The presented method is not commercially available. Due to regulatory reasons, its future availability cannot be guaranteed. The Siemens Multitom Rax is not available in all countries, its future availability cannot be guaranteed.

REFERENCES

[1] Dobbins, J. T., "Tomosynthesis imaging: at a translational crossroads," *Medical physics* **36**(6), 1956–1967 (2009).

[2] Duryea, J., Dobbins, J., and Lynch, J., "Digital tomosynthesis of hand joints for arthritis assessment," *Medical physics* **30**(3), 325–333 (2003).

[3] Flynn, M. J., McGee, R., and Blechinger, J., "Spatial resolution of x-ray tomosynthesis in relation to computed tomography for coronal/sagittal images of the knee," in [*Proc. SPIE*], **6510**, 65100D (2007).

[4] Ha, A. S., Lee, A. Y., Hippe, D. S., Chou, S.-H. S., and Chew, F. S., "Digital tomosynthesis to evaluate fracture healing: prospective comparison with radiography and ct," *American Journal of Roentgenology* **205**(1), 136–141 (2015).

[5] Machida, H., Yuhara, T., Tamura, M., Ishikawa, T., Tate, E., Ueno, E., Nye, K., and Sabol, J. M., "Whole-body clinical applications of digital tomosynthesis," *Radiographics* **36**(3), 735–750 (2016).

[6] Dobbins, J. T. and Godfrey, D. J., "Digital x-ray tomosynthesis: current state of the art and clinical potential," *Physics in medicine and biology* **48**(19), R65 (2003).

[7] Deschênes, S., Charron, G., Beaudoin, G., Labelle, H., Dubois, J., Miron, M.-C., and Parent, S., "Diagnostic imaging of spinal deformities: reducing patients radiation dose with a new slot-scanning x-ray imager," *Spine* **35**(9), 989–994 (2010).

[8] Horbaschek, H., "Universal x-ray device having a pivotally mounted radiator and a displaceably mounted detector," (June 1 2004). US Patent 6,742,929.

[9] Shibata, K., Notohara, D., and Sakai, T., "Parallel-scanning tomosynthesis using a slot scanning technique: Fixed-focus reconstruction and the resulting image quality," *Medical physics* **41**(11) (2014).

[10] Luckner, C., Mertelmeier, T., Maier, A., and Ritschl, L., "Towards full-body x-ray images," in [*Bildverarbeitung für die Medizin 2018*], Springer (2018).

[11] Mertelmeier, T., Orman, J., Haerer, W., and Dudam, M. K., "Optimizing filtered backprojection reconstruction for a breast tomosynthesis prototype device," in [*Proc. SPIE*], **6142**, 61420F (2006).

[12] Lauritsch, G. and Härer, W. H., "A theoretical framework for filtered backprojection in tomosynthesis," in [*Proc. SPIE*], **3338**(2), 1127–1137 (1998).

[13] Reiser, I. and Glick, S., [*Tomosynthesis imaging*], Taylor & Francis (2016).

[14] Zhou, J., Zhao, B., and Zhao, W., "A computer simulation platform for the optimization of a breast tomosynthesis system," *Medical physics* **34**(3), 1098–1109 (2007).

[15] Steckmann, S., Knaup, M., and Kachelrieß, M., "High performance cone-beam spiral backprojection with voxel-specific weighting," *Physics in Medicine & Biology* **54**(12), 3691 (2009).

[16] Segars, W. P., Mahesh, M., Beck, T. J., Frey, E. C., and Tsui, B. M., "Realistic ct simulation using the 4d xcat phantom," *Medical physics* **35**(8), 3800–3808 (2008).

[17] Fieselmann, A., Steinbrener, J., Jerebko, A. K., Voigt, J. M., Scholz, R., Ritschl, L., and Mertelmeier, T., "Twin robotic x-ray system for 2d radiographic and 3d cone-beam ct imaging," in [*SPIE Medical Imaging*], 97830G–97830G, International Society for Optics and Photonics (2016).

[18] Li, B., Avinash, G. B., Uppaluri, R., Eberhard, J. W., and Claus, B. E., "The impact of acquisition angular range on the z-resolution of radiographic tomosynthesis," in [*International Congress Series*], **1268**, 13–18, Elsevier (2004).

[19] Kunze, H., Haerer, W., Orman, J., Mertelmeier, T., and Stierstorfer, K., "Filter determination for tomosynthesis aided by iterative reconstruction techniques," in [*9th International Meeting on Fully Three-Dimensional Image Reconstruction in Radiology and Nuclear Medicine*], 309–312 (2007).